Substrate and Surfactant Effects on the Glass−Liquid Transition of Thin Water Films

Ryutaro Souda*

Nanoscale Materials Center, National Institute for Materials Science, 1-1 Namiki, Tsukuba, Ibaraki 305-0044, Japan

Received: March 24, 2006; In Final Form: June 28, 2006

Temperature-programmed time-of-flight secondary ion mass spectrometry (TP-TOF-SIMS) and temperature-programmed desorption (TPD) have been used to perform a detailed investigation of the adsorption, desorption, and glass−liquid transition of water on the graphite and Ni(111) surfaces in the temperature range 13−200 K. Water wets the graphite surface at 100−120 K, and the hydrogen-bonded network is formed preferentially in the first monolayer to reduce the number of nonbonding hydrogens. The strongly chemisorbed water molecules at the Ni(111) surface do not form such a network and play a role in stabilizing the film morphology up to 160 K, where dewetting occurs abruptly irrespective of the film thickness. The surface structure of the water film formed on graphite is fluctuated considerably, resulting in deweting at 150−160 K depending on the film thickness. The dewetted patches of graphite are molecularly clean, whereas the chemisorbed water remains on the Ni(111) surface even after evaporation of the film. The abrupt drop in the desorption rate of water molecules at 160 K, which has been attributed to crystallization in the previous TPD studies, is found to disappear completely when a monolayer of methanol is present on the surface. This is because the morphology of supercooled liquid water is changed by the surface tension, and it is quenched by termination of the free OH groups on the surface. The surfactant methanol desorbs above 160 K since the hydrogen bonds of the water molecules are reconstructed. The drastic change in the properties of supercooled liquid water at 160 K should be ascribed to the liquid−liquid phase transition.

1. Introduction

Glassy water is ubiquitous in nature, and an understanding of its properties is important in many research fields, such as astrophysics, environmental science, and cryobiology. The surface of water ice has also received much attention especially in terms of its role in ozone depletion in Antarctic stratosphere. Despite the extensive studies, however, there remain significant controversies in the kinetics of the glass−liquid transition and crystallization of water. The glass-transition temperature, T_g, of water has been considered to be 136 K from the calorimetric study,[1] but it has been claimed that T_g should be reassigned to 160−165 K from the comparison of the T_g-scaled heat capacity between water and other inorganic glasses.[2,3] The latter was supported by the computer simulation[4] and dielectric study[5] as well. Recently, the origins of these two characteristic temperatures have been explained as the kinetics of the glass−liquid transition,[6] i.e., the translational diffusion commences at 136 K and then the morphological change of the film takes place typically at 160−165 K after some aging time. However, it is still an open question whether the supercooled liquid water, if any, is a thermodynamic extension of normal water or a distinct phase.

The glass-transition temperature defines the onset of molecular diffusion, so that the crystallization also occurs above T_g. The crystallization of amorphous solid water (ASW), which is deposited by gas phase water molecules at a cold substrate, has been studied extensively by isothermal desorption spectroscopy (ITDS)[7−9] and temperature-programmed desorption (TPD).[10−14] These studies assume that the phase transition is accompanied by a change in the vapor pressure: a drop in the desorption rate in the ITDS spectrum, as well as a bump in the TPD spectrum, has been explained by crystallization of ASW into cubic ice Ic. The crystallization has been reported to occur in a temperature range from 130 to 160 K, where the desorption rate of water molecules decreases by a factor of 3−100. Of particular interest is how the properties of the ASW films, such as glass transition and crystallization, are affected by the substrates, especially in terms of their hydrophilicity and hydrophobicity. The ITDS study claimed that crystallization temperature on the hydrophilic Pt(111) substrate is significantly higher than the hydrophobic graphite substrate,[8,9] and the origin of the different nucleation temperature was discussed. In this respect, it is also reported that the UV irradiation promotes crystallization of ASW due to photoexcited charge carriers formed in the graphite substrate[15] and that the initial sticking coefficient of the water molecules is much below unity at 100−120 K on the hydrophobic octane films.[16]

In the present paper, we employ temperature-programmed time-of-flight secondary ion mass spectrometry (TP-TOF-SIMS) and TPD to study how the adsorption/desorption behaviors and wetting/dewetting kinetics of the water molecules are influenced by the hydrophoicity/hydrophilicity of the substrates. The water film formed on the graphite surface is compared with that on the Ni(111) surface, and the effect of the monolayer of methanol adsorbed on the water film is investigated. In the previous studies, we have discussed the glass-transition kinetics of water on the Ni(111) surface,[6] but the conclusion that the supercooled liquid water is dominant above T_g conflicts significantly to that of ITDS and TPD studies mentioned above. Here, we compare the results between TP-TOF-SIMS and TPD to resolve such a discrepancy and clarify the origin of the reported "phase transition" of water. Moreover, the critical thickness for the

* E-mail: SOUDA.Ryutaro@nims.go.jp.

10.1021/jp061831f CCC: $33.50
Published on Web 08/16/2006

emergence of the bulk properties is determined in terms of the glass−liquid transition of water on the graphite substrate.

2. Experiment

Experiments were performed in an ultrahigh vacuum (UHV) chamber that has a base pressure below 1×10^{-8} Pa. The UHV system was equipped with an electron-impact-type ion source, a linear-TOF tube, and a differentially pumped quadrupole mass spectrometer for TPD. To minimize charging and damage of a surface, a pulsed He^+ beam (1.5 keV) with a low incident flux (0.1 nA/cm^2) was used for TP-TOF-SIMS measurements. The spectrum was taken continuously at a time interval of 30 s, and the temperature was ramped at a rate of 5 K/min. The sample of highly oriented pyrolytic graphite (HOPG) was purchased from Matsushita Electric Co. It was cleaved in air using the "Scotch Tape" method.[14] The Ni(111) substrate was cut from a single-crystal rod and polished mechanically to a mirror finish. The HOPG sample was mounted on a Ta sheet that was spot-welded to a sample holder made of Ta. To ensure a good thermal contact, the sample was clamped tightly with Ta strips. The Ni(111) sample was spot-welded to the Ta holder using a Ni sheet. The samples were inserted in the UHV chamber via a load-lock system. Cooling of the sample was achieved by thermal contact between the mirror-finished faces of the Ta holder and a sapphire plate that was attached to the copper block cooled to 13 K by means of a closed-cycle helium refrigerator. Heating was achieved by electron bombardment from behind through a square hole opened in the sapphire plate. The HOPG and Ni(111) samples, respectively, were heated in UHV at 1000 and 1200 K for cleaning and annealing. Water and methanol were admitted into the chamber through high-precision leak valves. They were deposited on the surface by backfilling the UHV chamber. In the TOF-SIMS experiments, the coverage of the adsorbed molecules was determined from the evolution curves of sputtered ion intensities as a function of exposure:[17] the 1 monolayer (ML) of water was formed on the Ni(111) surface with the exposure at around 2.5 langmuir ($1\ \text{L} = 1 \times 10^{-6}$ Torr s). On the hydrophobic surfaces, the initial sticking probability of water might be less than unity above 100 K.[16] Therefore, the water film on the HOPG surface was characterized tentatively by exposure of water molecules. TOF-SIMS and TPD spectra were recorded at the same heating rate.

3. Experimental Results

Figure 1 shows mass spectra of positive ions from the water-adsorbed (a) Ni(111) and (b) graphite surfaces measured at 100 K. No appreciable cations are sputtered from the clean Ni and graphite surfaces, and the ion intensities increase upon adsorption of 5-L water molecules. From the water-adsorbed Ni(111) surface, the bare and hydrated Ni^+ ions, $Ni^+(H_2O)_n$ ($n = 0-5$), are sputtered predominantly relative to the ions sputtered from the water film (H^+ and $H^+(H_2O)_n$). The fact that no Ni^+ ions are sputtered from the clean Ni(111) surface indicates that the sputtered Ni^0 atoms are ionized during collision with the water molecules on the way out from the surface and some H_2O molecules are coordinated.[17] In the case of graphite surface, some reacted ions, such as CH_n^+ ($n = 0-2$) and H_nCO^+ ($n = 1-3$), are sputtered. They are thought to be caused by the reactions between the sputtered energetic C^0 atoms and the H_2O molecule. The HCO^+ and $Ni^+(H_2O)$ ions cannot be sputtered through a thick water film, so that their emission provides evidence not only for wetting of thin water films on the substrates but also for possible dewetting of the thick water films

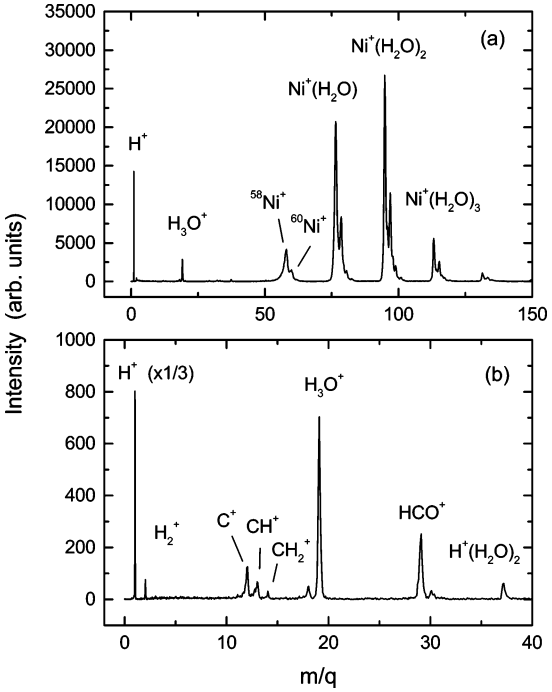

Figure 1. Secondary positive-ion mass spectra from the water-adsorbed (a) Ni(111) and (b) graphite surfaces. The H_2O molecules (5 L) were deposited on the surfaces at 100 K.

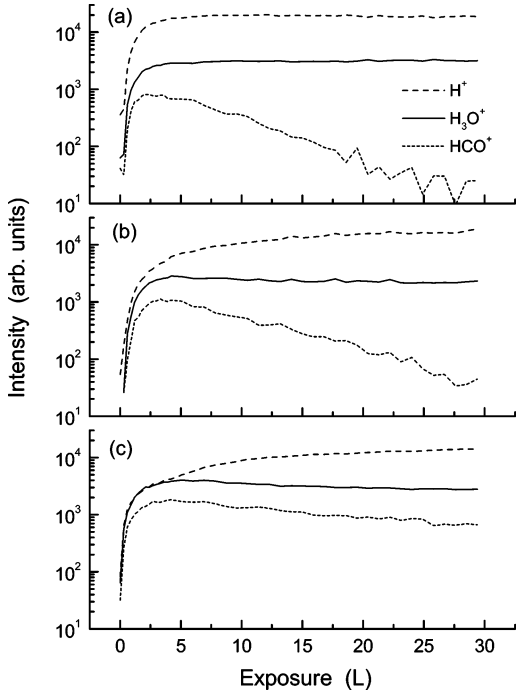

Figure 2. Intensities of the H^+, H_3O^+, and HCO^+ ions sputtered from the water-adsorbed graphite surface as a function of the exposure of the H_2O molecules. The measurements were made at different surface temperatures of (a) 13 K, (b) 100 K, and (c) 120 K.

by increasing temperature. On this basis, we discuss the water−substrate interactions at the molecular level.

Figure 2 shows evolution curves of H^+, H_3O^+, and HCO^+ ions as a function of exposure of the H_2O molecules. The measurements were made at (a) 13 K, (b) 100 K, and (c) 120 K. The H^+ and H_3O^+ intensities are saturated at around 2.5 L where the HCO^+ ion is peaked in intensity. The evolution curves at 100 K are basically the same as those at 13 K except that the evolution of the H^+ ion and decay of the HCO^+ ion are more

gradual at 100 K. These tendencies are promoted when water is deposited on graphite at 120 K. It is reasonable to assume that the sticking coefficient of the water molecules is unity at 13 K and no 2D or 3D islands are grown due to the limited diffusion length on the surface. This film is rather characterized by porosity[18] or a large number of hydrogen-bond imperfections between the water molecules. It should be noted that the evolutions of the H_3O^+ and HCO^+ ions below 2.5 L are independent of the surface temperature, indicating that the initial sticking coefficient of the water molecules is unity. The slower decay of the HCO^+ ion in the multilayer coverage regime should be ascribed to the formation of the 3D islands on the monolayer-adsorbed graphite surface, suggesting the Stranski−Krastanov-type growth mode on the graphite surface though the film is not crystalline at all as will be discussed later. The H^+ ion should be caused by bond breaking of the "free" hydroxyl group with a partly ionic character, so that the high H^+ intensity from the porous ASW film deposited at 13 K is reasonable. The preferential hydrogen-bond formation between the adsorbed water molecules should be responsible for the suppression of the initial H^+ evolution at the higher-temperature surfaces. It is also likely that the water molecules tend to stick by pointing their free OH group toward the graphite surface. In any case, such structures are specific to the first monolayer and the increased H^+ intensity with exposure suggests that the randomly oriented amorphous film grows in the multilayer regime. This finding is consistent with the theoretical calculation that predicts the formation of a hexagonal hydrogen-bonded network in the first monolayer of water on the graphite (0001) surface.[19] On the Ni(111) surface, no such behaviors are observed in the evolution curves of the H^+ intensities at temperatures between 13 and 120 K (the results are not shown explicitly). Probably, the chemisorbed water molecules are bound to the Ni(111) surface with the free hydrogens up. In the following, the film is characterized by the estimated thickness rather than exposure since the sticking coefficients of water on both graphite and Ni(111) are thought to be unity.

To gain more insights into the mobility of water molecules, the temperature evolutions of the secondary ion intensities were measured. In Figure 3 are compared the ion intensities from the water-adsorbed (a) graphite and (b) Ni(111) surfaces: The 4 ML of H_2O were deposited on the surfaces at 100 K and then the temperature was increased at the same rate. There exist significant differences in the ion evolutions between the graphite and Ni(111) surfaces. The H^+ intensity from the graphite surface exhibits a marked temperature dependence whereas it is almost constant below 160 K from the Ni(111) surface. No such temperature dependencies are observed in the H_3O^+ intensities for both surfaces. These results suggest that the hydrogen-bond structures of the water molecules are more changeable on the graphite surface. All ion intensities drop at around 147 K on the graphite surface due to the morphological change of the film: above this temperature, the HCO^+ ion disappears completely though the H^+ and H_3O^+ ions remain. As already described, the emission of the HCO^+ ion can be an experimental measure of wettability of the graphite surface, so that this result indicates that the complete dewetting takes place at 150 K. On the Ni(111) surface, the $Ni^+(H_2O)$ intensity (the H^+ intensity) increases (decreases) steeply due to dewetting at 160 K. This is because the opened patches of the Ni(111) surface after dewetting are not clean and are covered with the chemisorbed water molecules. They remain on the surface even after the evaporation of the water multiplayer at 170 K. Thus, the TOF-SIMS experiments reveal the hydrophobicity, hydrophilicity, and wettability of the surfaces at the molecular level.

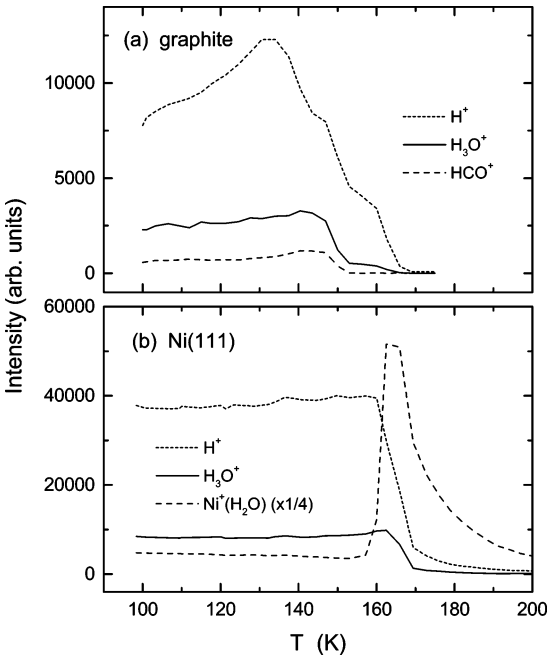

Figure 3. TP-TOF-SIMS intensities from the (a) graphite and (b) Ni-(111) surfaces on which the 4 ML (10 L) of water molecules were deposited at 100 K.

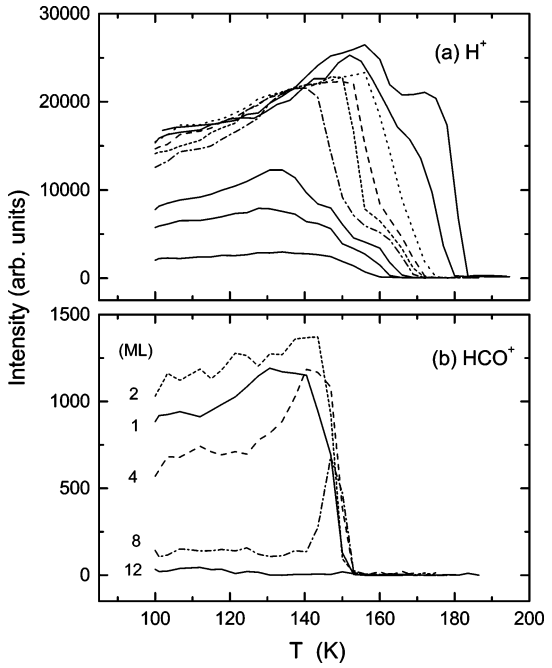

Figure 4. TP-TOF-SIMS intensities of (a) H^+ and (b) HCO^+ ions from the water-deposited graphite surface. Water molecules were adsorbed at 100 K. The H^+ intensities from the water films with coverages 1, 2, 4, 8, 12, 16, 20, 40, and 80 ML and the HCO^+ intensities from 1 to 12 ML films are plotted as a function of surface temperature. With increasing coverage, the H^+ intensity increases and its drop and cutoff, respectively, due to the dewetting and evaporation of the film shift to higher temperatures continuously. No HCO^+ ions are emitted from the water films thicker than 16 ML.

The dewetting behaviors of the water films are further investigated as a function of coverage and temperature. The experimental results for the graphite surface are shown in Figure 4. The HCO^+ ions are emitted from the thin water films with the thickness less than 12 ML (see also Figure 2b). For such

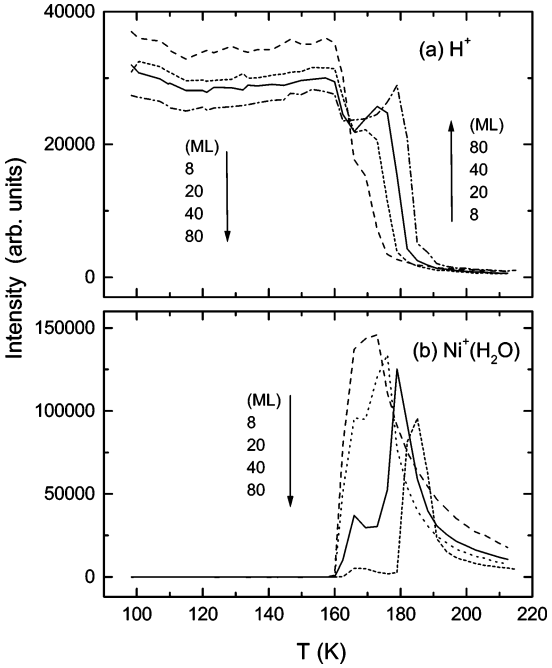

Figure 5. TP-TOF-SIMS intensities of (a) H^+ and (b) $Ni^+(H_2O)$ ions from the water-deposited Ni(111) surface. The water molecules with coverage from 8 to 80 ML were deposited on the clean Ni(111) surface at 100 K.

films, the dewetting temperatures are fixed at 150 K as revealed by the HCO^+ intensity. The water molecules tend to diffuse on the surface prior to dewetting as typically seen for the 4- and 8-ML films that exhibit the evolution of the HCO^+ ion above 130−140 K. The absence of the HCO^+ ion for the thicker films (>12 ML) does not necessarily exclude the possibility of dewetting because it implies that the film raptures without passing through the transient thickness range enabling the HCO^+ emission. The resulting water droplets have a small contact area with the graphite surface. The occurrence of dewetting can also be recognized in the H^+ intensity. The H^+ intensity has a fixed decay edge at around 150 K for the thin films (<8 ML). The edge shifts to the higher temperature with increasing the film thickness and finally reaches 160 K. The H^+ intensity decays considerably after dewetting because of the low density of the droplets: they increase in number and size with increasing coverage and, finally, a continuous granular film which covers the entire graphite surface results from a thick water film.

In the case of the Ni(111) surface shown in Figure 5, on the other hand, the decay edge of the H^+ ion, together with the onset for evolution of the $Ni^+(H_2O)$ ion, is almost pinned at 160 K independent of the film thickness. With increasing coverage, a peak of the $Ni^+(H_2O)$ intensity splits into a hump at the dewetting temperature and a peak at the evaporation temperature. The hump at 160 K disappears for the films thicker than 150 ML (not shown explicitly) due to the formation of the continuous granular film without exposure of the Ni(111) substrate. Even for the water film as thick as 1600 ML, the surface morphology changes at 160 K, as evidenced by the presence of a dip in the H^+ intensity. Therefore, the morphological change of the film at 160 K is a pure bulk phenomenon. The thinner the film is, the higher the H^+ intensity becomes for $T < 160$ K. The opposite tendency is observed for the water films on the graphite surface as seen in Figure 4. This is caused by the preferential formation of the 3D islands on the graphite substrate (see Figure 2b), as well as the substrate effect on the sputtering yield. The presence of the heavy substrate beneath

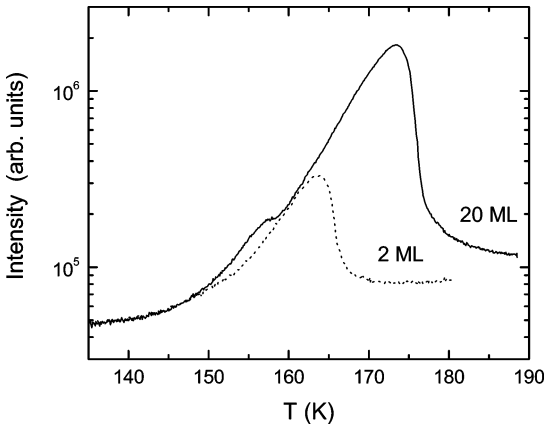

Figure 6. TPD spectra of water ($m/q = 18$) from the 2-ML (dotted line) and 20-ML (solid line) water films deposited on the graphite substrate at 100 K.

the light molecular films enhances the sputtering yield due to the evolution of the collision cascade toward the surface and the contribution of the backscattered He^0 atoms. This was confirmed from the computer simulation based on the SRIM code.[20]

The morphological change of the film should affect the desorption rate of the water molecules. Typical TPD spectra of water from the graphite surface are shown in Figure 6. The desorption of the water molecules commences at around 140 K. In the case of the 20 ML film shown by a solid line, a hump occurs at 158 K due to the abrupt drop in the desorption rate at higher temperatures. This temperature corresponds approximately to the dewetting temperature of the water film observed in the TOF-SIMS experiment. The hump becomes unclear especially for the thinner films where the dewetting temperature shifts from 160 to 150 K (see Figure 4). The TPD traces, when plotted with a logarithmic scale, can be characterized by two separated lines corresponding to the different desorption rates before and after dewetting. Therefore, dewetting of the thinner films can be discussed in comparison with these reference lines. In the case of the 2 ML film (a dotted line), the desorption rate apparently changes at around 150−152 K due to dewetting. Thus, it is concluded that the changes in the desorption rate of water molecules is related to the morphological change of the films.

The previous TOF-SIMS study[17] revealed that the monolayer of alcohols and carbonic acids stays on the surface of the ASW without incorporation in the bulk and it quenches dewetting of the film. Such a surfactant effect has been investigated by TPD as well. The TPD spectra of water and methanol from the methanol (1 ML) adsorbed H_2O film (40 ML) are shown in Figure 7 by solid lines. The hump of the water TPD spectrum disappears completely due to the presence of methanol, and the shape of the spectrum fits well to that from the pure water film (a broken line) after dewetting occurs. This result clearly shows that the methanol has essentially the same effect on the desorption rate of water molecules as the dewtted water film. It should be noted that the desorption rate of methanol increases abruptly above 158 K, indicating that the properties of water change drastically at this temperature.

4. Discussion

The phase transition from the ASW to the crystalline ice Ic has been discussed on the basis of the TPD and ITDS studies.[7−15] They are based on the assumption that the desorption rate of the water molecules from the crystalline phase may be

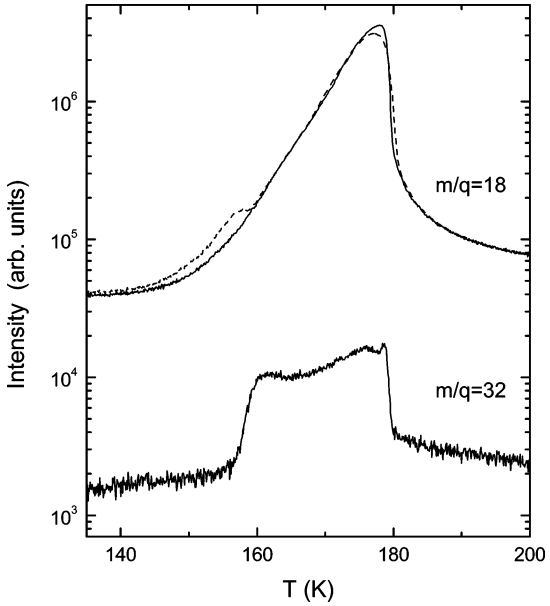

Figure 7. TPD spectra of water ($m/q = 18$) and methanol ($m/q = 32$) from the methanol (1 ML) adsorbed water film (40 ML) deposited at 100 K. Also shown by a broken line is the TPD spectrum from the pure water film (40 ML) without methanol.

much smaller than that from the amorphous phase, so that the changes in the desorption rates can be ascribed uniquely to crystallization. In reality, however, this assumption is not established at all because the desorption rate is dependent on many other factors, such as the morphology of the film and the presence of surfactants, as demonstrated in the present study. One possible explanation for the change in the desorption rate is the simple decrease in the surface area associated with the morphological change. Microscopically, moreover, the desorption rate should be related to the surface energy which is thought to be determined by the structure of the hydrogen-bonded water molecules at the surface. The drop of the TOF-SIMS H^+ intensity after dewetting, as well as the surfactant effect of methanol, supports this view. The crystallization is believed to occur for all exposures in which multilayers are present, but the hump in the TPD spectra can only be observed for limited exposures.[14] Moreover, the quenching of bulk crystallization by the monolayer of methanol is hardly explicable. The surfactant effect observed in our TOF-SIMS and TPD experiments is expected for the fluidized films. Thus, the "phase transition" discussed in the previous ITDS and TPD studies is not due to crystallization, but it should be ascribed to the formation of supercooled liquid water. It is apparent that the long-range order like crystallization cannot be discussed by the ITDS and TPD data alone, and more reliable crystallographic data are necessary. The electron diffraction study[21] concluded that at most 30% of water molecules crystallize in the temperature range 140−210 K. In the calorimetric study, moreover, it is known that the crystallization exotherm occurs in a broad temperature range from 150 to 180 K but no abrupt behavior at 160 K is observed at all.[1] As regards the glass−liquid transition, it has been depicted that the expected endotherm at 136 K[1] is too small to assign the real glass−liquid transition, and this behavior leads to the significant confusion.[2−4] In the previous paper, we depicted that a small hump toward the endothermic side observed at around 165 K should be ascribed to the real glass-transition endotherm that is hindered in the huge crystallization exotherm.[6] Therefore, it is likely that crystallites coexist with supercooled liquid, but the possibility of homogeneous nucleation to ice Ic should be excluded. This picture seems to explain most of the existing experimental results consistently. Since TOF-SIMS reveals the dynamical behaviors of the water molecules, it clarifies the nature of supercooled liquid water rather than coexisting crystallites.

It should be noted that the dewetting temperature (160−165 K) is considerably higher than the onset of molecular diffusion at $T_g = 136$ K.[17] This phenomenon can be explained in terms of decoupling.[6] One of the most remarkable characteristics of supercooled "fragile" liquid is that the inverse proportionality between the translational diffusion coefficient and viscosity is broken at $T < 1.2\ T_g$ (163 K for water with $T_g = 136$ K);[22] the viscosity of deeply supercooled liquid is higher by as much as 2 orders of magnitude than that expected from the molecular diffusion. Thus, the supercooled liquid water is classified as fragile liquid, as evidenced by the ultraviscous nature at around T_g and the delayed evolution of fluidity.

The present study also revealed how the bulk property of the water film evolves from the strongly substrate-dependent monolayer regime. The dewetting temperature of thin water films deposited on the graphite surface (150 K) is lower than that on the Ni(111) surface (160 K). The deviation should be ascribed to the different bonding nature of the water molecules at the interface. No chemical bond is formed between water and graphite. The water molecules physisorb with their dipole parallel to the surface and the hexagonal hydrogen-bonded network is formed preferentially to reduce the number of free OH groups.[19] The predicted geometry shows no preference of nonbonding H atoms up and down, but the strong suppression of the experimental H^+ intensity at the monolayer coverage regime may suggest the preference of the hydrogen-down orientation. On the Ni(111) surface, the water molecules are immobilized due to the chemisorption via the lone-pair electrons of oxygen. Such water molecules at the interface act as a template, so that the formation of the hexagonal hydrogen-bonded network is prohibited and dewetting of the water films is induced only by the surface tension irrespective of the film thickness. On the other hand, the lower dewetting temperature on the graphite surface may be induced by the instability of the interface structure, originating from the mobility of the water molecules above T_g. In the latter, a question arises as to why the dewetting temperature deviates from $T_g = 136$ K even for the 2 ML water film. This phenomenon may be elucidated in terms of decoupling mentioned above. In reality, however, the decoupling is caused by the kinetics of the glass−liquid transition: The isothermal TOF-SIMS experiment revealed that the thick water films dewet the Ni(111) surface even at 135−140 K after a considerably long aging time (∼10−15 min).[6] Therefore, the dewetting temperatures of 150 and 160 K, respectively, for the graphite and Ni(111) surfaces, have less physical meaning because they rather correspond to the different aging times for the glass−liquid (or liquid−liquid) transition. In this respect, the results of the ITDS study[8,9] are still instructive if the term "crystallization" is taken as dewetting. As expected, the dewetting time of the water films on the Pt(111) surface is much longer than that on the graphite surface in the temperature range 145−150 K.

The critical thickness for the appearance of the pure bulk properties in the water films can be assigned to 20−40 ML from the dewetting behavior of water on the graphite surface as seen in Figure 4a. The temperature dependence of the H^+ intensity is conspicuous for thinner films and still remains for the considerably thick water films deposited on the graphite surface as compared to the Ni(111) surface. The continuous

increase of the H^+ intensity up to the dewetting temperature implies that the water molecules are reorganized at the surface. Such reorganization seems to occur even below T_g, where the translational diffusion of molecules should be quenched. One possible explanation of this behavior is the rotational relaxation of the molecules which occurs at temperatures lower than T_g (∼120 K).[23] In any case, the absence of such behaviors for the water films on the Ni(111) surface indicates that the structural instability at the water−graphite interface influences the surface molecular orientation beyond the considerably thick water films. The instability of thin water films may be explained in terms of spinodal dewetting:[24,25] unstable growth of capillary waves driven by attractive dispersion forces across the film causes surface fluctuations, and the expectation time for dewetting varies strongly with the film thickness. Thus, the surface structure of the water film can be influenced by the instability of the water−graphite interface. The preferential 3D-island formation on the graphite surface at 120 K (see Figure 2c) suggests that the water molecules coming from the gas phase have long diffusion lengths on the surface, which may be related to the presence of the hexagonal hydrogen-bonded network in the first monolayer or the reduced number of free OH groups at the surface.

The properties of supercooled liquid water change drastically at 160 K. This phenomenon may be explained by liquid−liquid transition of water. The ultraviscous liquid water (136 K < T < 160 K) is connected to ASW (T < 136 K) without any structural discontinuity, so that the surfactant methanol can stay on the surface up to 160 K. On the other hand, a considerable reconstruction of hydrogen bonds occurs during dewetting, as evidenced by the fact that the methanol molecules terminating free OH groups at the surface are forced to desorb abruptly. The break in the properties of supercooled water at 160 K has been evidenced by the interactions with the other solute species. For example, the alkenes, which are accommodated in the bulk of the ASW film, also survive in the ultraviscous liquid phase above T_g, but they are released abruptly at around 160 K.[26] According to the second critical point hypothesis,[27] supercooled liquid water consists of two distinct phases, termed low density liquid (LDL) and high density liquid (HDL). The former has ordered hydrogen bonds with an open structure whereas the latter is characterized by disordered, weak hydrogen bonds. LDL is characterized by a tetrahedrally structured liquid and accommodates hydrophobes in the bulk.[28] Therefore, the ultraviscous nature of deeply supercooled water (136 K < T < 160 K) should be ascribed to LDL. The dehydration of alkanes at 160 K suggests that LDL transforms to another liquid phase.[26] Recently, this assumption is supported by the fact that LiCl dissolves in the supercooled liquid water only after the morphological change of the film occurs.[29] The resulting LiCl solutions are highly concentrated and are thought to be identical to the quenched LiCl solutions. The high (poor) solubility of electrolytes (hydrophobes) is characteristic of normal water (LDL + HDL), so that the supercooled liquid phase above 160 K should link directly to normal water at room temperature.

5. Conclusion

The strong substrate effects are found to exist in the initial adsorption structure and dewetting kinetics of the water molecules on the graphite surface in comparison with the results on the Ni(111) surface. The water molecules wet the graphite surface with initial sticking probability of unity in the temperature range from 13 to 120 K. There exist a large number of hydrogen-bond imperfections in the film deposited at 13 K, as estimated from the sputtered H^+ intensity. The hydrogen-bonded network of water molecules is formed preferentially on the graphite surface in the first monolayer when deposited at 100 and 120 K. This occurs to reduce the number of the nonbonding hydrogen atoms. On the Ni(111) surface, no such hydrogen bond structures are formed in the first monolayer due to chemisorption of the molecules. The dewetting temperature of water on Ni(111) is basically fixed at 160 K over a wide thickness range from 4 to 1600 ML since the chemisorbed water molecules play a role as a template. Because of the absence of such a template, the structure of the water films formed on graphite is more fluctuated and, hence, the thin water films (<15 ML) dewet the graphite surface at lower temperature (150 K). The dewetting temperature of water on graphite increases with thickness and finally reaches 160 K for 20−40 ML films, where the pure bulk property of water is thought to emerge.

From the comparison between the TOF-SIMS and TPD experiments, the abrupt change in the desorption rate, which was previously assigned to crystallization by the TPD and ITDS studies, is found to be caused by dewetting of the supercooled water film. The hump in the desorption rate of the water molecules disappears when the surface is covered with the monolayer of methanol. Such a surfactant effect is hardly explained by bulk crystallization. As regards the glass−liquid transition of water, the dewetting temperature (160 K) is higher than the conventional T_g of 136 K because the diffusion coefficient and the viscosity are decoupled in the deeply supercooled regime (T < 1.2 T_g). The surfactant methanol molecules terminating the free OH groups are released above 160 K due to the reorganization of the hydrogen-bond structures of the surface and bulk water molecules. The liquid−liquid transition is responsible for the drastic change in the properties of water before and after dewetting, indicating that two distinct liquid phases coexist in the deeply supercooled regime.

References and Notes

(1) Johari, G. P.; Hallbrucker, A.; Mayer, E. *Nature* **1987**, *330*, 552.
(2) Velikov, V.; Borick, S.; Angell, C. A. *Science* **2001**, *294*, 2335.
(3) Yue, Y.; Angell, C. A.; *Nature* **2004**, *427*, 717.
(4) Giovambattista, N.; Angell, C. A.; Sciortino, F.; Stanley, H. E. *Phys. Rev. Lett.* **2004**, *93*, 047801.
(5) Minoguchi, A.; Richert, R.; Angell, C. A. *Phys. Rev. Lett.* **2004**, *93*, 215703.
(6) Souda, R. *Chem. Phys. Lett.* **2005**, *415*, 146.
(7) Smith, R. S.; Huang, C.; Wong, E. K. L.; Kay, B. D. *Surf. Sci.* **1996**, *367*, L13.
(8) Lofgren, P.; Ahlstrom, P.; Ghakarov, D. V.; Lausmaa, J.; Kasemo, B. *Surf. Sci.* **1996**, *367*, L19.
(9) Lofgren, P.; Ahlstrom, P.; Lausma, J.; Kasemo, B.; Chakarov, D. *Langmuir* **2003**, *19*, 265.
(10) Smith, R. S.; Huang, C.; Wong, E. K. L.; Kay, B. D. *Phys. Rev. Lett.* **1997**, *79*, 909.
(11) Smith, R. S.; Kay, B. D. *Nature* **1999**, *398*, 788.
(12) Dohnalek, Z.; Ciolli, R. L.; Kimmel, G. A.; Stevenson, K. P.; Smith, R. S.; Kay, B. D. *J. Chem. Phys.* **1999**, *110*, 5489.
(13) Smith, R. S.; Huang, C.; Kay, B. D. *J. Phys. Chem. B* **1997**, *101*, 6123.
(14) Bolina, A. S.; Wolff, A. J.; Brown, W. A. *J. Phys. Chem. B* **2005**, *109*, 16836.
(15) Chakarov, D.; Kasemo, B. *Phys. Rev. Lett.* **1998**, *81*, 5181.
(16) Linderoth, T. R.; Zhdanov, V. P.; Kasemo, B. *Phys. Rev. Lett.* **2003**, *90*, 156103.
(17) Souda, R. *Phys. Rev. B* **2004**, *70*, 165412.
(18) Stevenson, K. P.; Kimmel, G. A.; Smith, R. S.; Kay, B. D.; *Science* **1999**, *283*, 1505.
(19) Sanfelix, P. C.; Holloway, S.; Kolasinski, K. W.; Darling, G. R. *Surf. Sci.* **2003**, *532*−*535*, 166.
(20) Ziegler, J. F.; Biersack, J. P.; Littmark, U. In *The Stopping and Range of Ions in Solids*; Pergamon Press: New York, 1985.
(21) Jenniskens, P.; Banham, S. F.; Blake, D. F.; McCoustra, M. R. S. *J. Chem. Phys.* **1997**, *107*, 1232.

(22) Debenedetti, P. G.; Stillinger, F. H. *Nature* **2001**, *410*, 259 and references therein.
(23) Fisher, M.; Devlin, J. P. *J. Phys. Chem.* **1995**, *99*, 11584.
(24) Thiele, U.; Mertig, M.; Pompe, W. *Phys. Rev. Lett.* **1998**, *80*, 2869.
(25) Yerushalmi-Rozen, R.; Kerle, T.; Klein, J. *Science* **1999**, *285*, 1254.
(26) Souda, R. *J. Chem. Phys.* **2004**, *121*, 8676.
(27) Mishima, O.; Stanley, H. E. *Nature* **1998**, *396*, 329.
(28) Paschek, D. *Phys. Rev. Lett.* **2005**, *94*, 217802.
(29) Souda, R. *J. Phys. Chem. B* **2006**, *110*, 14787.